REFERENCES AND NOTES

1. D. Gospodarowicz, in *Mediators in Cell Growth and Differentiation*, R. J. Ford, A. L. Maizel, Eds. (Raven, New York, 1985), p. 109.
2. D. Gospodarowicz, *Methods Enzymol.* in press.
3. Y. Shing *et al.*, *Science* **223**, 1296 (1984); R. R. Lobb and J. W. Fett, *Biochemistry* **23**, 6295 (1984).
4. Basic FGF is probably identical to β-heparin binding growth factor (HGFβ), tumor angiogenesis factor (TAF), eye-derived growth factor I (EDGFI), β-retina-derived growth factor (βRDGF), cartilage-derived growth factor (CDGF), cationic hypothalamus-derived growth factor (cHDGF), and to a component of macrophage-derived growth factor (MDGF). Acidic FGF is probably identical to endothelial cell growth factor (ECGF), α-heparin binding growth factor (HGFα), eye-derived growth factor II (EDGFII), α-retina-derived growth factor (αRDGF), and anionic hypothalamus derived growth factor (αHDGF). [A. Baird, F. Esch, D. Gospodarowicz, R. Guillemin, *Biochemistry* **24**, 7855 (1985); J. Courty *et al.*, *Biochimie* **67**, 265 (1985); P. A. D'Amore and M. Klagsbrun, *J. Cell Biol.* **99**, 1545 (1984); R. Sullivan and M. Klagsbrun, *J. Biol. Chem.* **260**, 2399 (1985); M. Klagsbrun and Y. Shing, *Proc. Natl. Acad. Sci. U.S.A.* **82**, 805 (1985); A. Baird, P. Mormède, P. Böhlen, *Biochem. Biophys. Res. Commun.* **126**, 358 (1985); K. A. Thomas, M. Rios-Candelore, S. Fitzpatrick, *Proc. Natl. Acad. Sci. U.S.A.* **81**, 357 (1984); T. Maciag, T. Mehlman, R. Friesel, A. B. Schreiber, *Science* **225**, 932 (1984); A. B. Schreiber *et al.*, *J. Biol. Chem.* **101**, 1623 (1985); and the references in (*3*)].
5. D. Gospodarowicz, H. Bialecki, T. K. Thakral, *Exp. Eye Res.* **28**, 501 (1979); R. R. Lobb, E. A. Alderman, J. W. Fett, *Biochemistry* **24**, 4969 (1985); D. Gospodarowicz, J. Cheng, G.-M. Lui, A. Baird, P. Böhlen, *Proc. Natl. Acad. Sci. U.S.A.* **81**, 6963 (1984).
6. K. A. Thomas *et al.*, *Proc. Natl. Acad. Sci. U.S.A.* **82**, 6409 (1985).
7. F. Esch *et al.*, *ibid.*, p. 6507.
8. G. Gimenez-Gallego *et al.*, *Science* **230**, 1385 (1985); F. Esch *et al.*, *Biochem. Biophys. Res. Commun.* **133**, 554 (1985).
9. M. Jaye *et al.*, *Nucleic Acids Res.* **11**, 2325 (1983); S. Anderson and I. B. Kingston, *Proc. Natl. Acad. Sci. U.S.A.* **80**, 6838 (1983); R. Derynck, A. B. Roberts, M. E. Winkler, E. Y. Chen, D. V. Goeddel, *Cell* **38**, 287 (1984); B. Greenberg, personal communication.
10. A. Mergia *et al.*, in preparation.
11. T. V. Huynh, R. A. Young, R. W. Davis, in *DNA Cloning: A Practical Approach*, D. M. Glover, Ed. (IRL Press, Oxford, 1985), vol. 1, pp. 49–78.
12. P. Mormède, A. Baird, P. Pigeon, *Biochem. Biophys. Res. Commun.* **128**, 1108 (1985).
13. M. Kozak, *Nucleic Acids Res.* **12**, 857 (1984).
14. R. Derynck *et al.*, *Nature (London)* **316**, 701 (1985); J. Battey *et al.*, *Cell* **34**, 779 (1983); T. J. Dull, A. Gray, J. S. Hayflick, A. Ullrich, *Nature (London)* **310**, 777 (1984); T. Collins *et al.*, *ibid.* **316**, 748 (1985).
15. R. Sullivan, J. A. Smith, M. Klagsbrun, *J. Cell Biol.* **101**, 108a (1985); R. Lobb *et al.*, *J. Biol. Chem.* **261**, 1924 (1986).
16. G. von Heijne, *Eur. J. Biochem.* **133**, 17 (1983).
17. C. J. March *et al.*, *Nature (London)* **315**, 641 (1985); P. E. Auron *et al.*, *Proc. Natl. Acad. Sci. U.S.A.* **81**, 7907 (1984).
18. R. P. Woychik *et al.*, *Nucleic Acids Res.* **10**, 7197 (1982).
19. W. I. Wood *et al.*, *Nature (London)* **312**, 330 (1984).
20. W. I. Wood, J. Gitschier, L. A. Lasky, R. M. Lawn, *Proc. Natl. Acad. Sci. U.S.A.* **82**, 1585 (1985).
21. J. Messing and J. Vieira, *Gene* **19**, 269 (1982).
22. F. Sanger, S. Nicklen, A. R. Coulson, *Proc. Natl. Acad. Sci. U.S.A.* **74**, 5463 (1977).
23. P. Thomas, *ibid.* 77, 5201 (1980); H. Lehrach, D. Diamond, J. M. Wozney, H. Boedtker, *Biochemistry* **16**, 4743 (1977).

24. We thank J. Iwasa and T. Scheuermann for synthesizing the oligonucleotides, F. Rottman (Case Western Reserve) for the bovine genomic library, J. Miller for help with the DNA sequencing, B. Greenberg for compiling the bovine codon choice table, E. Stoelting for the artwork, L. Fritz and K. Talmadge for their critical comments on the manuscript, and C. Remington, M. Matsumura, and E. Pond for preparing the manuscript.

10 March 1986; accepted 5 May 1986

A Cusp Singularity in Surfaces That Minimize an Anisotropic Surface Energy

JEAN E. TAYLOR AND JOHN W. CAHN

A mathematical proof shows that a surface with a cusp-shaped singularity can arise from minimizing an anisotropic surface free energy for a portion of a crystal surface. Such cusps have been seen on crystal surfaces but usually have been interpreted as being the result of defects or nonequilibrium crystal growth. Our result predicts that they can occur as equilibrium or near-equilibrium phenomena. It also enriches the mathematical theory of minimal surfaces.

THE MATHEMATICAL MODELING OF shapes that minimize total crystal surface free energy has a long history. Initially, only isotropic fluids (as represented by soap films, for example) were considered (*1*). This led to the mathematical subject of minimal surfaces, which is currently very active (*2*). But from Gibbs (*3*) onward, it has been recognized that the surface free energy per unit area of the surface of a crystal of fixed orientation is a function of the unit normal directions of the surface (*4*). The anisotropy arises from the fact that the atomic structure of the surface can be very different in different unit normal directions.

Unlike liquid drops, crystals can have edges and corners as part of their equilibrium shapes. In our investigation of such singularities (*5*) and their evolution, we encountered a problem that suggested that a cusp-shaped singularity could occur in an energy-minimizing surface. The present report is the mathematical proof that it is so, together with some experimental evidence. With the orientation of the solid phase or phases fixed in space, and with fixed temperature, pressure, and chemical potentials, the surface free energy per unit area, γ, is a function that maps unit vectors $\mathbf{n}$ to positive numbers. The normals $\mathbf{n}$ are chosen to point from the crystal to the other phase. The nature of both phases determines γ. The other phase can be vapor, liquid, or another crystal, perhaps of the same material but with another orientation. It is convenient to describe γ by means of its Wulff shape (also called its equilibrium crystal shape)

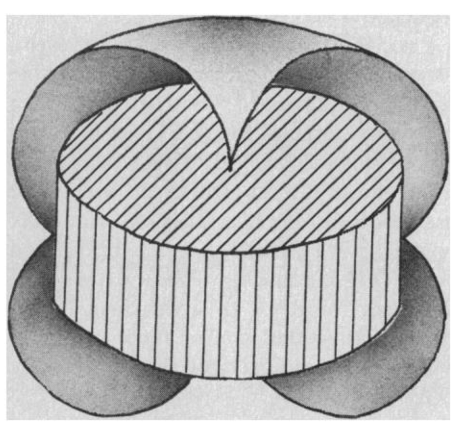

Fig. 1. A cylindrical W. Any γ that satisfies the conditions in expressions 2 through 4 will have this W as its Wulff shape. The back half of the polar plot of one such γ is drawn around W.

$$W = \{\mathbf{x} \in \mathrm{R}^3 : \mathbf{x} \cdot \mathbf{n} \leq \gamma(\mathbf{n}) \text{ for each unit vector } \mathbf{n}\} \qquad (1)$$

That is, W is the set composed of all the vectors $\mathbf{x}$ in 3-space for which $\mathbf{x} \cdot \mathbf{n} \leq \gamma(\mathbf{n})$. W is the shape of least surface energy for the crystal of fixed volume entirely embedded in the other phase (*6–9*).

The surface free energy function γ that we will use for the examples and proofs below is any function whose Wulff shape is a vertical right circular cylinder (Fig. 1). Normalizing γ if necessary, we can and do assume that

$$\gamma(\mathbf{n}) = 1 \qquad (2)$$

for each horizontal unit vector $\mathbf{n} = (n_1, n_2, 0)$ and

$$\gamma((0,0,1)) = \gamma((0,0,-1)) = \gamma_v \qquad (3)$$

Since W is a cylinder,

$$\gamma(\mathbf{n}) \geq (1 - n_3^2)^{1/2} + \gamma_v |n_3| \qquad (4)$$

for each of the other unit vectors $\mathbf{n} = (n_1, n_2, n_3)$.

Description of a cusp-shaped singularity. Consider a surface S, as in Fig. 2, which consists of a vertical cliff face with a horizon-

J. E. Taylor, Mathematics Department, Rutgers, the State University of New Jersey, New Brunswick, NJ 08903.
J. W. Cahn, Center for Materials Science, National Bureau of Standards, Gaithersburg, MD 20899.

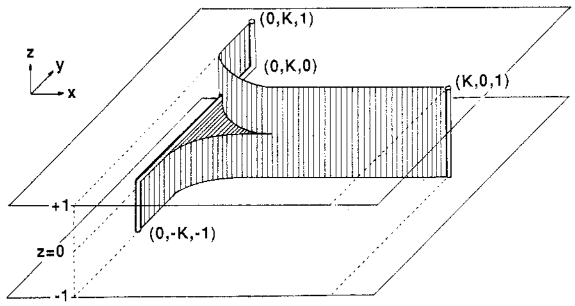

Fig. 2. The solution to the partially free boundary problem with $h = 0$ described in the text, shown in an isometric view. The fixed parts of the boundary are indicated as if they were rods. The free parts lie in the upper and lower planes.

tal shelf half way up on the left that peters out in the middle. On the right, the cliff is a vertical straight wall; on the left, the top part curves back and the bottom part curves forward, with the walls remaining vertical except for the shelf. S thus has a cusp in the curve separating the vertical walls from the horizontal shelf.

A variational problem with a cusp. In the following, we consider a special type of problem that reveals the reason that cusps occur in minimizing surfaces. We show that, in the class of surfaces that have part of their boundary fixed (as described below) and part constrained only to lie in the pair of parallel planes $z = 1$ and $z = -1$, there is a unique surface that minimizes the integral of γ; this surface has a cusp-shaped singularity in it. Figure 2 illustrates that surface for one such partially fixed and partially free boundary. We will first prove this result with a number of assumptions and a particular fixed part of the boundary. Then we will solve it in a more general case with the same assumptions, and finally we will use geometric measure theory to show that our assumptions are justified.

Let K be any number greater than $1/\gamma_v$. In the initial problem, the fixed part of the boundary consists of a horizontal line at $x = 0$, $z = 0$ that runs from $y = -K$ to $y = K$, together with three vertical line segments, one from the point $(0,K,0)$ to the point $(0,K,1)$, one from $(0,-K,0)$ to $(0,-K,-1)$, and one from $(K,0,-1)$ to $(K,0,1)$. We will show that the free part of the boundary in each plane is a quarter of a circle together with line segments, as shown in Fig. 2.

We assume that there are functions $f_1(x) \geq 0 \geq f_2(x)$ such that the minimizing surface S is composed of a horizontal part $H = \{(x,y,0)\colon\ f_2(x) < y < f_1(x)\}$ and two vertical parts $S^+ = \{(x,y,z)\colon\ 0 \leq z < 1$ and either $0 < x < K,\ y = f_1(x)$ or $x = 0,\ f_1(0) < y < K\}$ and $S^- = \{(x,y,z)\colon\ -1 < z \leq 0$ and either $0 < x < K,\ y = f_2(x)$ or $x = 0, f_2(0) > y > -K\}$. At the minimum, a small deformation of f_1 around any x should result in equal and opposite changes in the area of S^+ compared to γ_v times the area of H. Since the radius of curvature R_1 of the graph of f_1 at x is the limit, as such deformations go to zero, of the change in area (under the graph of f_1 compared to its deformation) divided by the change in arc length, we conclude that R_1 must be equal to $1/\gamma_v$ wherever $f_1(x) > 0$ and $x \neq 0$. Similarly, R_2 must equal $1/\gamma_v$ wherever $f_2(x) < 0$, and the graphs of f_1 and f_2 must meet the x- and y-axes smoothly. (The identical solution is obtained through the standard calculus of variations; one can also recognize the two-dimensional capillarity problem lurking here, which also gives circular arcs.)

A related family of problems has a similar partially fixed boundary, except that the height h of the horizontal line is not zero. The same argument then yields that the radius of curvature R_1 of the top part at the shelf should be constantly $(1 - h)/\gamma_v$ and R_2 should be constantly $(1 + h)/\gamma_v$, provided that the problem is set up so that the portions of the circles stay away from the end points of the horizontal line (a convenient way to achieve this is to put the vertical line segment connecting the two planes at $x = K(1 - h^2)^{1/2}$, $y = Kh$ rather than at $x = K$, $y = 0$ as before). A similar argument shows that, where the top part of S and the bottom part coincide, the radius of curvature must be infinite and thus the coincidence curve must be a straight line. Both parts must again attach to the boundary line at $x = 0$, $z = h$ with a continuous tangent plane and to each other with a common tangent plane, which requires (see Fig. 3) that the slope $\tan \alpha$ of the common tangent line in the plane $z = h$ be defined by $R_1 \cot[(\pi/2 - \alpha)/2] = R_2 \cot[(\pi/2 + \alpha)/2]$ so that $\tan \alpha = h/(1 - h^2)^{1/2}$.

To complete the proof, it remains only to verify our various assumptions. The most general context in which to do so is geometric measure theory. Briefly, a solution in at least the varifold (infinitesimally corrugated) sense exists simply by taking a limit of a subsequence of a minimizing sequence [see (*10*)] (such limits exist since the minimizing sequence can be made to stay within a bounded radius of the origin, and it naturally has bounded area). The support S of the limit varifold is a "(γ,δ)-restricted set" and can thus be strongly approximated by continuously differentiable two-dimensional surfaces (*10*). By inequality 4 above, the surface free energy of S is at least γ_v times the area of the orthogonal projection of S onto a horizontal plane, plus the integral, from $z = -1$ to $z = 1$, of the length of S at height z. Thus energy is not decreased by sloping. One is therefore best off by having S consist of a part of a horizontal plane (at height h, since the horizontal part of the fixed boundary is there) together with vertical parts, each horizontal slice of which has one of the two possible minimum lengths, depending on whether it is above or below that horizontal plane. To find S, we must thus find two one-dimensional rectifiable curves C_1 and C_2 in the plane $z = h$, with the boundary of C_1 equal to the points $(K(1 - h^2)^{1/2}, Kh)$ and $(0,K)$, and the boundary of C_2 equal to the points $(K(1 - h^2)^{1/2}, Kh)$ and $(0,-K)$, such that $(1 - h) \cdot \text{length}(C_1) + (1 + h) \cdot \text{length}\ (C_2) + \gamma_v \cdot$ (area of the region between C_1 and C_2) is minimized. Finally, since C_1 and C_2 are rectifiable, they are each a collection of closed loops together with a simple curve connecting their boundary points; since they minimize the above expression, they are in fact each a simple curve. One now analyzes radii of curvature as before to conclude that C_1 and C_2 are the curves found previously.

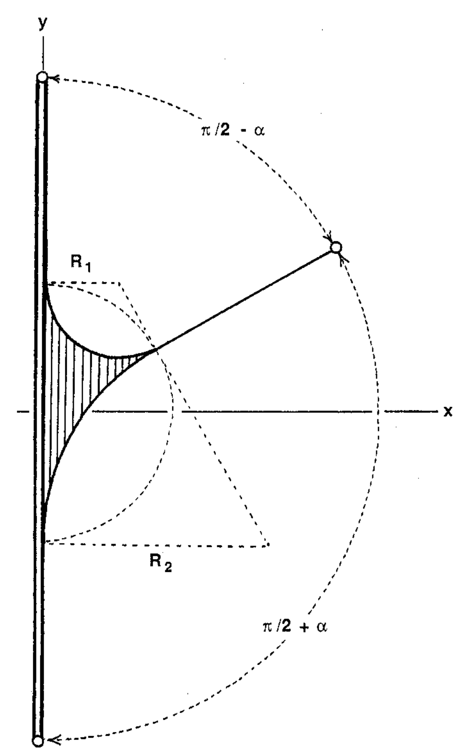

Fig. 3. The solution to the partially free boundary problem with $h = 1/2$, shown from above. The vertical fixed parts of the boundary are shown as small circles.

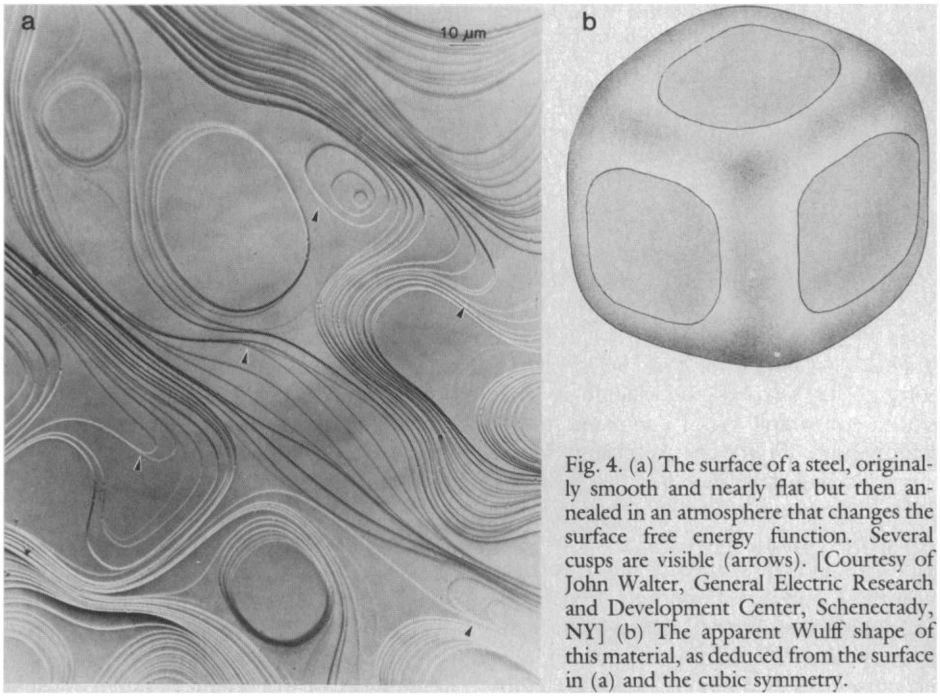

Fig. 4. (a) The surface of a steel, originally smooth and nearly flat but then annealed in an atmosphere that changes the surface free energy function. Several cusps are visible (arrows). [Courtesy of John Walter, General Electric Research and Development Center, Schenectady, NY] (b) The apparent Wulff shape of this material, as deduced from the surface in (a) and the cubic symmetry.

Fixed boundaries and surfaces with cusps. The prescribed boundary problem is a useful way of focusing attention on one part of a larger physical surface. It also can be realized in many different experimental schemes, even with solid surfaces. To construct mathematically examples of the cusp in such completely fixed boundary problems we fix smooth curves C_1 and C_2 in the planes $z = 1$ and $z = -1$, respectively, such that their projections onto the plane $z = 0$ have a common line segment on the right; we adjoin a vertical line segment joining the end points of C_1 and C_2 on the right and a horizontal line segment (at height h) on the left, with its ends bent up and down to meet the left end points of the curves. The radii of curvature of C_1 can be any values greater than or equal to $(1 - h)/2\gamma_V$; they need not be equal, as long as the curve bends in only one direction. Similarly, those of C_2 can be any values at least $(1 + h)/2\gamma_V$ in the opposite direction. The surface S with a horizontal ledge terminating in a cusp in a surface that is otherwise vertical will again be the unique minimizing surface (*11*). The proof can also be extended to show that minimizing surfaces with cusps exist whenever W is any cylinder, not necessarily circular or right or having any particular symmetry (*12*).

Experimental evidence for the cusp. Such cusps abound on crystal surfaces. They can be shown not to be due to screw dislocations emerging to the surface or to other bulk defects, and they occur persistently in crystal surfaces that have had long annealing times. For example, the surface of the silicon-iron crystal of Fig. 4a is well equilibrated by an anneal of 8 hours at 1250°C in a controlled atmosphere of argon [as described in (*13*)]. This surface is essentially flat, but with many shelves [(100) facets] and short sloping walls separating them. Several cusps are visible, where a shelf peters out in the middle of a wall. Using the overall cubic symmetry of the material and the rounded square outlines of the figure, we deduce that the Wulff shape for the surface energy of the surface in Fig. 4a is a slightly distorted sphere with six caps sliced off, as in Fig. 4b [such Wulff shapes have been calculated theoretically (*14*)]. The surface is clearly not at an overall equilibrium: many features, including the cusps, violate the barrier constructs (*5*) in the large. Because diffusion over distances of the size of these violations is required to remove these nonequilibrium features, they remain for long times. But the surface can be at essential equilibrium with respect to local atomic rearrangements in small enough regions (of radius less than the height difference between shelves). And even though the cusps are over a large scale a kinetic phenomenon in this case, in other experiments they need not be: surfaces with cusps can be absolutely surface energy–minimizing (as shown above) and hence cusps can be an equilibrium phenomenon.

Generalization: We conjecture that minimizing surfaces with cusp-shaped singularities can exist whenever γ is such that its Wulff shape has a flat facet with a curved sharp edge. When W has a sharp curved planar edge but no flat facets, a plausible argument can be made that the cusp cannot exist in a surface having only the normals of W. Varifold surfaces (surfaces with infinitesimal corrugations, or hill-and-valley structures) seem to arise instead if one tries to force a cusp to occur, provided that strict inequality holds in the formula analogous to Eq. 1. Presumably edge energies will also need to be included in the formulation of the problem to predict what would be seen in actual materials with that type of surface energy function.

A phenomenon related to this cusp has been seen in soap films with a partially free boundary (*15*). Here a wire emerges from the top of a sheet of glass, spirals around one of its edges, and reattaches on the bottom side so that the projection of the wire on the plane of the glass crosses itself. If the wire is positioned correctly, the curve where the soap film contacts the upper surface of the glass and the curve where it contacts the lower surface meet in a cusp at the edge of the glass. Since in this case there is zero energy associated with the surface along the glass between the contact curves, we can convert this problem to an anisotropic surface energy problem with a completely fixed boundary by assigning zero energy to the downward-pointing normal, constant energy to normals in the upper hemisphere, adding a line segment to connect the boundary ends, and removing the glass. W is now the upper half ball, and we expect the same surface as the soap film plus the horizontal ledge terminating in a cusp to be minimizing.

We have demonstrated mathematically that the cusp can be part of an energy-minimizing surface of a crystal whose surface energy function γ is such that its Wulff shape is a cylinder. The cusp differs from the various possible first-order singularities (ones where there is no tangent plane) that we have cataloged (*5*) in that there is a tangent plane to the surface at the point of the cusp. Much work still needs to be done to determine what happens for other surface energy functions.

The frequent observation of cusps in real crystal surfaces needs to be reinterpreted in view of the knowledge that such features can be part of equilibrium surface shapes, and therefore are not necessarily a result of defects or growth history.

REFERENCES AND NOTES

1. See J. C. Maxwell [in *Encyclopaedia Britannica*, ed. 11 (1911), vol. 5, pp. 256–275] for a history.
2. There are two different approaches to minimal surfaces today, that of differential geometry and that of geometric measure theory. For examples of the former, see the volume *Seminar on Differential Geometry*, S. T. Yau, Ed. [*Ann. Math. Studies* **102** (1982)]. For examples of the latter, see the volume *Geometric Measure Theory and the Calculus of Variations*, W. K. Allard and F. J. Almgren, Jr., Eds. [*Proc. Symp. Pure Math.* **44** (1986)].
3. J. W. Gibbs, *The Collected Works of J. W. Gibbs* (Longmans, Green, New York, 1928).

4. The interdisciplinary use of language by mathematicians and metallurgists can be a problem. Two-dimensional mathematical surfaces are used to represent surfaces, interfaces, and grain boundaries of crystals. We reserve the word "boundary" to mean the one-dimensional curves (straight or otherwise) that are spanned by portions of surfaces. In this report, therefore, a grain boundary is a surface (and not a "boundary").
5. J. E. Taylor and J. W. Cahn, *Acta Metall.* **34**, 1 (1986).
6. G. Wulff, *Z. Krystallogr. Mineral.* **34**, 499 (1901).
7. A. Dinghas, *Z. Kristallogr.* **105**, 304 (1944).
8. C. Herring, *Phys. Rev.* **82**, 87 (1951).
9. J. E. Taylor, *Bull. Am. Math. Soc.* **84**, 568 (1978); see also J. E. Taylor, in *Geometric Measure Theory and the Calculus of Variations* [in (2)].
10. F. J. Almgren, Jr., *Mem. Am. Math. Soc.* **4** (No. 165) (1976), pp. v–vii and 53–56.
11. The prescribed boundary problem allows one to use the technique of barriers to see directly that surface free energy cannot be decreased by having the surface slope or zigzag toward the middle. Any surface T composed of a horizontal half-plane and a vertical half-plane sharing their bounding line is uniquely minimizing since it is (a translation of) a tangent cone to the cylinder W or its central inversion (9). Therefore no minimizing surface S' can cross such a two–half-plane surface T on the interior of S'. A family of such T's brought up against the prescribed boundary from in front and above shows that any minimizing surface S' having the prescribed boundary must lie on or behind the top part of S and on or below the horizontal part of S. Similarly, a family of T's brought up against the boundary from in back and below the horizontal part of S shows that any such minimizing surface S' must lie on or in front of the lower part of S and on or above the horizontal part of S. Therefore, the horizontal part of S is pinned by T's from above and below and must be in each and every minimizing surface S' having the same boundary as S. The remainder of S' is thus split effectively into two pieces, a top one and a bottom one. It only remains to show that these pieces are the cylindrical parts of S. But this in turn follows from the assumption on the radii of curvature of C_1 and C_2 and the arguments made previously, since the surface free energy for each piece of S' is at least $2\gamma_v$ times the projected area of that piece plus the z-integral of the lengths of its intersection with horizontal planes. (The factor of 2 arises from the fact that, if there are noncylindrical parts in these remaining pieces, they will cover their projection on the horizontal plane at least twice.)
12. If W is a right cylinder, the above proof goes over fairly directly, though the integrals are more complicated; if W is not a right cylinder, one can do a linear transformation of space to convert W to a right cylinder, solve the problem, and transform back again.
13. C. G. Dunn and J. L. Walter, *Acta Metall.* **7**, 648 (1959).
14. C. Rottman and M. Wortis, *Phys. Rev. B* **29**, 328 (1984).
15. S. Hildebrandt and J. C. C. Nitsche, *Arch. Ration. Mech. Anal.* **79**, 189 (1982).
16. Supported in part by National Science Foundation grants MCS-8301869 and DMS-8502942. We also thank the Institute for Mathematics and Its Applications, University of Minnesota, Minneapolis, MN, and the Institute for Advanced Study, Princeton, NJ, for their support. The figures were drawn by F. J. Almgren, Jr.

19 December 1985; accepted 13 March 1986

The Generation of Insulin-Like Growth Factor-1–Sensitive Cells by Growth Hormone Action

KATHLEEN M. ZEZULAK AND HOWARD GREEN

Insulin-like growth factor-1 (IGF-1), a mitogenic polypeptide, is usually considered the sole effector by means of which growth hormone increases tissue mass. However, growth hormone, but not IGF-1, directly promotes the differentiation of cultured preadipocytes to adipocytes. Adipocytes newly differentiated from precursor cells in response to growth hormone were shown to be much more sensitive to the mitogenic effect of IGF-1 than the precursor cells. The result of IGF-1 action is therefore a selective multiplication of young differentiated cells (clonal expansion). This supports the concept of a dual effector system in which the preferred target cells of IGF-1 action are created by the direct action of growth hormone.

GROWTH HORMONE SPECIFICALLY promotes the differentiation of cloned lines of preadipose 3T3 cells into adipose cells (*1*). This is the result of a direct action of the hormone on the cells; IGF-1 (insulin-like growth factor-1 or somatomedin C), which has been regarded as an obligatory intermediate effector of the hormone in the promotion of growth (*2–4*), does not promote this differentiation (*5, 6*). To account for the direct and the IGF-mediated effects of growth hormone in animals, we proposed a dual effector theory (*7*) based on the concept that growth of tissues commonly occurs in two stages: (i) differentiated cells are formed from their precursors and (ii) the number of young differentiated cells is increased through limited multiplication (clonal expansion). The dual effector theory states that both stages are promoted by growth hormone: the first, directly by the hormone, and the second, indirectly, through its intermediate effector IGF-1. Although these two effects of the hormone cannot be easily distinguished in animal tissues, they can be distinguished in cell cultures. We show that cells with marked sensitivity to IGF-1 are produced by the prior action of growth hormone.

Preadipose 3T3-F442A cells were grown in 35-mm dishes containing the Dulbecco-Vogt modification of Eagle's medium supplemented with 5% cat serum and 0.5% calf serum. For experiments, cells grown to confluence in this medium were fed with modified conversion medium (*6*) containing 1.5% cat serum and 1.0% calf serum but lacking insulin to enable the cells to respond to IGF-1. The concentration of serum was the lowest compatible with good multiplication and adipose differentiation; the effects produced by added growth hormone and IGF-1 are increments over a relatively low background, some of which may be due to the presence of both proteins in the serum supplement.

The effect on adipose conversion produced by the addition of the two proteins is shown in Fig. 1. As the measure of differentiation, we used the activity of glycerophosphate dehydrogenase, a sensitive marker of the adipose phenotype (*8–10*). In the absence of added growth hormone, the differentiation of preadipose 3T3 cells was completely unresponsive to IGF-1, up to a concentration of 300 ng/ml. The cells did not develop glycerophosphate dehydrogenase, and although IGF-1 exerted a mitogenic action detectable by [^{14}C]thymidine incorporation (see below), it had no detectable effect on the total cell protein content per dish. No adipose cells were formed (Fig. 1D).

Human growth hormone promoted substantial differentiation even in the absence of added IGF-1, but when IGF-1 was added, the specific activity of cellular glycerophosphate dehydrogenase increased up to 4.5-fold (Fig. 1A). IGF-1 also substantially increased the protein content of the cultures in which the differentiation had been promoted by growth hormone (Fig. 1C). As a result, the total enzyme activity per culture undergoing adipose conversion increased up to tenfold after IGF-1 was added (Fig. 1B).

The combined effect of the hormone and IGF-1 could be the result of either more advanced differentiation within each adipose cell or an increase in the number of adipose cells. The proportions of adipose and nonadipose cells were therefore scored by counting cells containing or lacking fat droplets. This measurement is complicated by the fact that the addition of IGF-1 to growth hormone–treated cells increases the amount of lipid per fat cell. Using the dye Nile red, which is very specific and sensitive for lipid (*11*), to stain the living cells, we could easily identify fat cells containing small amounts of lipid. Cells exposed to IGF-1 alone did not acquire lipid droplets, but in growth hormone–treated cultures the addition of IGF-1 increased the proportion of adipose cells about 3.5-fold (Fig. 1D).

Department of Physiology and Biophysics, Harvard Medical School, Boston, MA 02115.